PCCP

Physical Chemistry Chemical Physics

# This paper is published as part of a PCCP Themed Issue on:

## "Molecules in Confined Spaces: The Interplay between Spectroscopy and Theory to develop Structure-Activity Relationships in the fields of Heterogeneous Catalysis, Sorption, Sensing and Separation Technology"

Guest Editor: Bert Weckhuysen

## Editorial Highlight

**Editorial Highlight: Molecules in confined spaces**
Robert A. Schoonheydt and Bert M. Weckhuysen, *Phys. Chem. Chem. Phys.*, 2009
**DOI:** 10.1039/b905015a

## Perspectives

**Nanoporous oxidic solids: the confluence of heterogeneous and homogeneous catalysis**
John Meurig Thomas, Juan Carlos Hernandez-Garrido, Robert Raja and Robert G. Bell, *Phys. Chem. Chem. Phys.*, 2009
**DOI:** 10.1039/b819249a

**Supported vanadium oxide in heterogeneous catalysis: elucidating the structure–activity relationship with spectroscopy**
Ilke Muylaert and Pascal Van Der Voort, *Phys. Chem. Chem. Phys.*, 2009
**DOI:** 10.1039/b819808j

**Correlating phase behaviour and diffusion in mesopores: perspectives revealed by pulsed field gradient NMR**
Rustem Valiullin, Jörg Kärger and Roger Gläser, *Phys. Chem. Chem. Phys.*, 2009
**DOI:** 10.1039/b822939b

## Communications

**Viscosity sensing in heated alkaline zeolite synthesis media**
Lana R. A. Follens, Erwin K. Reichel, Christian Riesch, Jan Vermant, Johan A. Martens, Christine E. A. Kirschhock and Bernhard Jakoby, *Phys. Chem. Chem. Phys.*, 2009
**DOI:** 10.1039/b816040f

**A small molecule in metal cluster cages: $H_2$@$Mg_n$ ($n$ = 8 to 10)**
Phillip McNelles and Fedor Y. Naumkin, *Phys. Chem. Chem. Phys.*, 2009
**DOI:** 10.1039/b819479c

## Papers

**Confinement effects on excitation energies and regioselectivity as probed by the Fukui function and the molecular electrostatic potential**
Alex Borgoo, David J. Tozer, Paul Geerlings and Frank De Proft, *Phys. Chem. Chem. Phys.*, 2009
**DOI:** 10.1039/b820114e

**Rotation dynamics of 2-methyl butane and *n*-pentane in MCM-22 zeolite: a molecular dynamics simulation study**
Shiping Huang, Vincent Finsy, Jeroen Persoons, Mark T.F. Telling, Gino V. Baron and Joeri F.M. Denayer, *Phys. Chem. Chem. Phys.*, 2009
**DOI:** 10.1039/b819334g

**Reactivity in the confined spaces of zeolites: the interplay between spectroscopy and theory to develop structure–activity relationships for catalysis**
Mercedes Boronat, Patricia Concepción, Avelino Corma, María Teresa Navarro, Michael Renz and Susana Valencia, *Phys. Chem. Chem. Phys.*, 2009
**DOI:** 10.1039/b821297j

**The influence of the chemical compression on the electric properties of molecular systems within the supermolecular approximation: the LiH molecule as a case study**
Anna Kaczmarek and Wojciech Bartkowiak, *Phys. Chem. Chem. Phys.*, 2009
**DOI:** 10.1039/b819346k

**Multinuclear gallium-oxide cations in high-silica zeolites**
Evgeny A. Pidko, Rutger A. van Santen and Emiel J. M. Hensen, *Phys. Chem. Chem. Phys.*, 2009
**DOI:** 10.1039/b815943b

**Metal–organic frameworks as high-potential adsorbents for liquid-phase separations of olefins, alkylnaphthalenes and dichlorobenzenes**
Luc Alaerts, Michael Maes, Monique A. van der Veen, Pierre A. Jacobs and Dirk E. De Vos, *Phys. Chem. Chem. Phys.*, 2009
**DOI:** 10.1039/b823233d

**Tetramethyl ammonium as masking agent for molecular stencil patterning in the confined space of the nano-channels of 2D hexagonal-templated porous silicas**
Kun Zhang, Belén Albela, Ming-Yuan He, Yimeng Wang and Laurent Bonneviot, *Phys. Chem. Chem. Phys.*, 2009
**DOI:** 10.1039/b819872c

**Photovoltaic activity of layered zirconium phosphates containing covalently grafted ruthenium tris(bipyridyl) and diquat phosphonates as electron donor/acceptor sites**
Laura Teruel, Marina Alonso, M. Carmen Quintana, Álvaro Salvador, Olga Juanes, Juan Carlos Rodriguez-Ubis, Ernesto Brunet and Hermenegildo García, *Phys. Chem. Chem. Phys.*, 2009
**DOI:** 10.1039/b816698f

**The characterisation and catalytic properties of biomimetic metal–peptide complexes immobilised on mesoporous silica**
Gerhard D. Pirngruber, Lukas Frunz and Marco Lüchinger, *Phys. Chem. Chem. Phys.*, 2009
**DOI:** 10.1039/b819678h

**Physisorption and chemisorption of alkanes and alkenes in H-FAU: a combined *ab initio*–statistical thermodynamics study**
Bart A. De Moor, Marie-Françoise Reyniers and Guy B. Marin, *Phys. Chem. Chem. Phys.*, 2009
**DOI:** 10.1039/b819435c

**Accelerated generation of intracrystalline mesoporosity in zeolites by microwave-mediated desilication**
Sònia Abelló and Javier Pérez-Ramírez, *Phys. Chem. Chem. Phys.*, 2009
**DOI:** 10.1039/b819543a

**Regio- and stereoselective terpene epoxidation using tungstate-exchanged takovites: a study of phase purity, takovite composition and stable catalytic activity**
Pieter Levecque, Hilde Poelman, Pierre Jacobs, Dirk De Vos and Bert Sels, *Phys. Chem. Chem. Phys.*, 2009
**DOI:** 10.1039/b820336a

**Probing the microscopic hydrophobicity of smectite surfaces. A vibrational spectroscopic study of dibenzo-*p*-dioxin sorption to smectite**
Kiran Rana, Stephen A. Boyd, Brian J. Teppen, Hui Li, Cun Liu and Cliff. T. Johnston, *Phys. Chem. Chem. Phys.*, 2009
**DOI:** 10.1039/b822635k

# The influence of the chemical compression on the electric properties of molecular systems within the supermolecular approximation: the LiH molecule as a case study

**Anna Kaczmarek*[a] and Wojciech Bartkowiak[b]**

*Received 3rd November 2008, Accepted 27th February 2009*
*First published as an Advance Article on the web 12th March 2009*
**DOI: 10.1039/b819346k**

The influence of the chemical compression on the electric properties of the model system is investigated. Two types of chemical environments are applied to exert pressure on the LiH molecule: nanotube-like and fullerene-like. The effects of two shapes of helium cavities onto the electric properties of the model system are discussed. The obtained results are compared to the data generated for the model spherical and cylindrical potentials by other authors.

## I. Introduction

The properties and the behaviour of the molecules enclosed in the cage can differ substantially from those of the gas phase or bulk. The weak interaction between the enclosed molecule and the cavity allows to finely tune the characteristics of the host system. Therefore this issue remains of interest in various branches of science: from catalytic effects on zeolites to the storage properties of the solid media.

The simplest way to mimic the confinement effects is to apply the model potential of the desired shape.[1–9] However, the chemical surrounding differs considerably from the one modelled by the impenetrable spherical or cylindrical wells, since the electron density distribution is not uniform in the whole space when one considers the chemical species built from atoms. Moreover, the harmonic oscillator potentials applied for this purpose act only on the electrons of the confined system. Thus, the model potentials are suitable for the introductory study giving some general aspects of the confinement effects, nevertheless they should be substituted by the real chemical species to reveal the true information about the molecular system.

In the last years growing interest can be noticed concerning the properties of the molecules enclosed in the chemical cages such as fullerene molecules, nanotubes, porous carbon materials, zeolites or crystals.[10–22] Stability of the enclosed system, its electro-optical properties, absorption and emission spectra, dielectric constants, magnetic properties or the reactivity have been shown to depend on the cavity surrounding the molecule.[6,10,12–35]

However, taking into account the size of the chemical species and the complexity of the topics mentioned above one has to carefully choose the computational methodology. When the weak molecular interactions come into play and the dispersion energy becomes an important component, the simple conventional density-functional methods should be used with a particular care. From the other side one can not easily afford the high-level *ab initio* calculations for the analysed systems. Hence the compromise between the accuracy and the computational efforts has to be established.

[a] *Faculty of Chemistry, Nicolaus Copernicus University, Gagarina 7, 87-100 Toruń, Poland. E-mail: teoadk@chem.uni.torun.pl*
[b] *Institute of Physical and Theoretical Chemistry, Wrocław University of Technology, Wybrzeże Wyspiańskiego 27, 50-370 Wrocław, Poland*

Therefore, the intermediate solution has been proposed: the investigation of the system of interest embedded in the model medium consisting of helium atoms.[10,25,36] The advantage of this approach is that the valence repulsion effects are taken into account in a natural way.

In the present study, the spatial confinement effects for the model LiH molecule are investigated. This simplest neutral heteroatomic molecule is frequently chosen as a model system for the benchmark calculations and the investigation of the issues of importance in the fields of methods development as well as in computational applications (for example in spectroscopy or non-linear optics) since it allows calculations using highly sophisticated techniques and large basis sets.[37–41]

Due to the simplicity of the chosen system, the set of the reference data is present in the literature just to mention some of the papers concerning the electro-optical properties of the isolated LiH[37–40] or its behaviour in the model axially symmetric harmonic oscillator potential.[41] The significant influence of the external axial harmonic potential has been observed on the dipole moment of the LiH molecule. Even more dramatic effects, such as the reduction of the equatorial components and heavy rise of the axial component can be noticed in the case of the dipole polarizability of LiH. These phenomena are due to the spatial restriction imposed on the electron density in the $x$ and $y$ directions in contrast to the only unconfined degree of freedom along the $z$ axis.[41] However the most pronounced results appear for the LiH geometry far from equilibrium—for the bond length equal to 3.015 a.u. all the differences are smaller than the most evident effects, although still not negligible.

The aim of the current work is to perform the comparison of the electric properties for the LiH molecule enclosed in the helium cavities of different shapes. The data obtained for the electric properties of the investigated complexes: dipole moment, dipole polarizability and first-order hyperpolarizability are related to the results generated with the model potentials to verify their general performance and the correspondence between the model and the chemical environment.

## II. Computational details

The test calculations were performed in the supermolecular manner for the LiH isolated molecule as well as for the

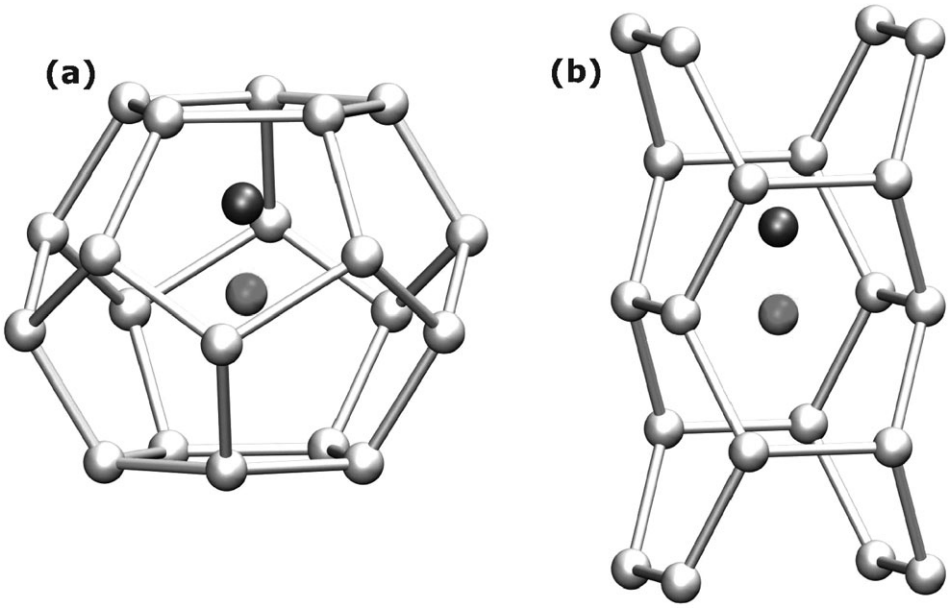


**Fig. 1** The investigated structures of LiH enclosed in the helium cages. (a) Spherical cavity and (b) cylindrical cavity. The white balls depicts helium atoms, lithium is light grey and hydrogen is dark grey.

LiH–helium complexes with two helium atoms. Supermolecular calculations were carried out within the HF, MP2, CCSD and CCSD(T) approximations with the series of Dunning correlation consistent basis sets aug-cc-pVXZ (X = D, T, Q). The Boys and Bernardi counterpoise scheme was applied to correct for the basis set superposition error. Obtained results justify the choice of the MP2/aug-cc-pVDZ method for further calculations.

In the scope of the present study two models were investigated: the first one, cylindrical, mimicking the nanotube environment and the other, spherical—simulating the fullerene cage. The helium tubes were generated on the basis of the structure of the carbon nanotube of the chirality (2,2) by changing the helium–helium distance to obtain the series of the tubules of the varying diameter.[42] Similarly, the helium fullerene-like series of cages is based on the $C_{20}$ structure. The tubular systems and the LiH bond are oriented along the $z$ axis. The structures of the investigated complexes are presented in Fig. 1.

All calculations were performed in GAMESS-US[43] program package. The equilibrium structure of the LiH molecule (bond distance 3.015 a.u.) was kept frozen during the calculations. The interaction energies and interaction-induced electric properties for the helium confinements were investigated within the MP2/aug-cc-pVDZ approach using the dimmer-centered basis set to avoid the basis set superposition errors. For comparison also the HF/aug-cc-pVDZ calculations were carried out, where necessary. Finite field technique was applied to estimate the corresponding energy derivatives with respect to the electric field.[44] The electric field of strength 0.001 a.u. was verified to provide numerically stable results.

In the supermolecular manner the interaction-induced property of the system, $\Delta P$, can be perceived as the difference of the property of the $N$-body complex and the sum of the properties of its constituents, $P_n$,

$$\Delta P = P_{\text{complex}} - \sum_{n=1}^{N} P_n. \tag{2.1}$$

However, equivalently one can consider the interaction-induced properties as the derivatives of the interaction energy with respect to the applied electric field:

$$\Delta\mu_i = -\left(\frac{\partial E_{\text{int}}}{\partial F_i}\right)_{F_i=0}, \tag{2.2}$$

$$\Delta\alpha_{ij} = -\left(\frac{\partial^2 E_{\text{int}}}{\partial F_i \partial F_j}\right)_{F_i=F_j=0}, \tag{2.3}$$

$$\Delta\beta_{ijk} = -\left(\frac{\partial^3 E_{\text{int}}}{\partial F_i \partial F_j \partial F_k}\right)_{F_i=F_j=F_k=0}, \tag{2.4}$$

respectively, for the interaction-induced dipole moment $\Delta\mu_i$, dipole polarizability $\Delta\alpha_{ij}$ and first-order hyperpolarizability $\Delta\beta_{ijk}$ where $i,j,k$ denote Cartesian components.

Since the polarizability and the first-order hyperpolarizabilityshow the anisotropic behaviour, the invariant average of polarizability

$$\alpha_{\text{ave}} = \tfrac{1}{3}(\alpha_{xx} + \alpha_{yy} + \alpha_{zz}) \tag{2.5}$$

and the vector component of the $\beta_{ijk}$ tensor projected on the axis of the dipole moment

$$\beta_z = \tfrac{3}{5}(\beta_{zxx} + \beta_{zyy} + \beta_{zzz}) \tag{2.6}$$

are investigated here.

The calculations for the helium enclosed LiH molecule were appended by the results of the interaction energy decomposition calculations followed by the estimations of the corresponding interaction-induced properties components within the variational-perturbational scheme[45–47] implemented in the EDS package connected to GAMESS-US.[48] According to this approach, the total interaction energy $\Delta E^{\text{MP2}}$ is partitioned into the Hartree–Fock $\Delta E^{\text{HF}}$ and correlation $\varepsilon^{(2)}_{\text{MP}}$ contributions. They can be further written as:

$$\Delta E^{\text{HF}} = \varepsilon^{(10)}_{\text{el}} + \varepsilon^{\text{HL}}_{\text{exch}} + \Delta E^{\text{HF}}_{\text{del}}, \tag{2.7}$$

and

$$\varepsilon^{(2)}_{\text{MP}} = \varepsilon^{(12)}_{\text{el},r} + \varepsilon^{(20)}_{\text{disp}} + \Delta E^{(2)}_{\text{exch,del}}, \tag{2.8}$$

 

respectively, where $\varepsilon_{el}^{(10)}$ denotes first-order electrostatic contribution, $\varepsilon_{exch}^{HL}$ is the Heitler–London exchange term, $\Delta E_{del}^{HF}$ collects the induction and charge-transfer effects, $\varepsilon_{el,r}^{(12)}$ stands for the correlation correction to the first-order electrostatic energy, the dispersion component is represented by $\varepsilon_{disp}^{(20)}$ and the sum of correlation corrections to the exchange and delocalization energy is expressed by $\Delta E_{exch,del}^{(2)}$.

## III. Results and discussion

### A Electron correlation: properties of the LiH molecule

The system of interest is built of two subsystems: the LiH molecule and the embedding helium atoms. The data available in the literature clearly indicate that in the case of the rare-gas systems the inclusion of electron correlation effects within the coupled-clusters approximation give the noticeable results only for the small internuclear distances. For the large interatomic separation electron correlation contributions become negligible.[49] However, for the second subsystem, the LiH molecule, the situation becomes more complicated. The inclusion of the electron correlation as well as the addition of the higher angular momentum basis functions is necessary to correctly describe the LiH molecule.[38] Nevertheless, considering

**Table 1** Axial components for the dipole moment, polarizability and first order hyperpolarizability of the LiH molecule; the correlation for all, not only valence, electrons included

| Level of theory | $\mu_z$/a.u. | $\alpha_{zz}$/a.u. | $\beta_{zzz}$/a.u. |
|---|---|---|---|
| SCF/aug-cc-pVDZ | −2.3713 | 20.80 | −370.8 |
| MP2/aug-cc-pVDZ | −2.3518 | 23.07 | −543.0 |
| CCSD/aug-cc-pVDZ | −2.3252 | 26.03 | −828.1 |
| CCSD(T)/aug-cc-pVDZ | −2.3249 | 25.95 | −825.0 |
| SCF/aug-cc-pVTZ | −2.3628 | 21.88 | −325.7 |
| MP2/aug-cc-pVTZ | −2.3413 | 23.60 | −454.8 |
| CCSD/aug-cc-pVTZ | −2.3100 | 26.06 | −672.6 |
| CCSD(T)/aug-cc-pVTZ | −2.3064 | 26.03 | −675.9 |
| SCF/aug-cc-pVQZ | −2.3620 | 21.89 | −312.5 |
| MP2/aug-cc-pVQZ | −2.3330 | 23.45 | −431.6 |
| CCSD/aug-cc-pVQZ | −2.3034 | 25.72 | −630.7 |
| CCSD(T)/aug-cc-pVQZ | −2.3017 | 25.81 | −641.3 |

**Table 2** Supermolecular interaction energy and interaction-induced electric properties for the LiH···($He_2$) complex

| Level of theory | $\Delta E$/ kcal mol$^{-1}$ | $\Delta\mu_z$/ a.u. | $\Delta\alpha_{zz}$/ a.u. | $\Delta\beta_{zzz}$/ a.u. |
|---|---|---|---|---|
| SCF/aug-cc-pVDZ | 8.80 | −0.1332 | −5.95 | 423.5 |
| MP2/aug-cc-pVDZ | 8.29 | −0.1515 | −7.30 | 578.1 |
| CCSD/aug-cc-pVDZ | 8.51 | −0.1761 | −9.33 | 842.6 |
| CCSD(T)/aug-cc-pVDZ | 8.42 | −0.1752 | −9.28 | 839.6 |
| SCF/aug-cc-pVTZ | 8.42 | −0.1381 | −5.78 | 404.1 |
| MP2/aug-cc-pVTZ | 7.34 | −0.1459 | −6.76 | 529.6 |
| CCSD/aug-cc-pVTZ | 7.53 | −0.1670 | −8.42 | 741.6 |
| CCSD(T)/aug-cc-pVTZ | 7.39 | −0.1656 | −8.37 | 738.9 |

**Table 3** Supermolecular interaction energy and interaction-induced electric properties for the tubular LiH–helium complex (helium–helium distance 2.5 Å)

| Level of theory | $\Delta E$/ kcal mol$^{-1}$ | $\Delta\mu_z$/ a.u. | $\Delta\alpha_{zz}$/ a.u. | $\Delta\beta_{zzz}$/ a.u. |
|---|---|---|---|---|
| SCF/aug-cc-pVDZ | 10.97 | −0.0595 | −7.79 | 310.7 |
| MP2/aug-cc-pVDZ | 9.27 | −0.0727 | −9.12 | 441.0 |
| CCSD/aug-cc-pVDZ | 9.40 | −0.0921 | −11.25 | 680.9 |

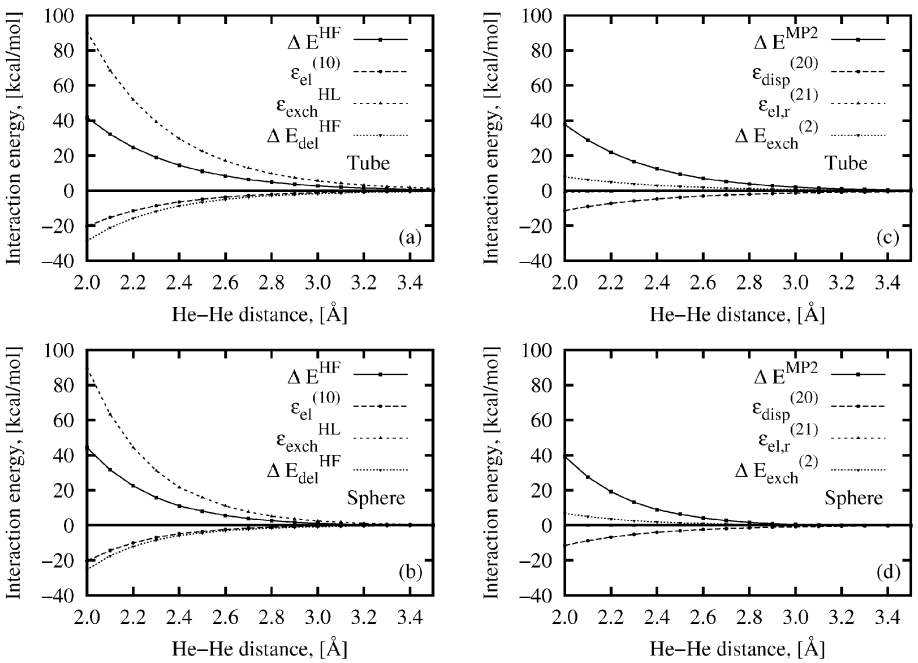


**Fig. 2** The interaction energy components for the tubular and spherical LiH–helium complex. All the values in kcal mol$^{-1}$. (a) First-order components: electrostatic, exchange and delocalization and total HF/aug-cc-pVDZ interaction energy for the tubular system. (b) First-order components: electrostatic, exchange and delocalization and total HF/aug-cc-pVDZ interaction energy for the spherical system. (c) Second-order components: dispersion, electrostatics and exchange and the total MP2/aug-cc-pVDZ interaction energy for the tubular system. (d) Second-order components: dispersion, electrostatics and exchange and the total MP2/aug-cc-pVDZ interaction energy for the spherical system.

**Table 4** The interaction energy components the LiH–helium cage complex calculated within the MP2/aug-cc-pVDZ approach via the variational-perturbational scheme

| He–He distance<br>Tubular cage | $\varepsilon_{el}^{(10)}$/<br>kcal mol$^{-1}$ | $\varepsilon_{exch}^{HL}$/<br>kcal mol$^{-1}$ | $\Delta E_{del}^{HF}$/<br>kcal mol$^{-1}$ | $\Delta E^{HF}$/<br>kcal mol$^{-1}$ | $\varepsilon_{el,r}^{(12)}$/<br>kcal mol$^{-1}$ | $\varepsilon_{disp}^{(20)}$/<br>kcal mol$^{-1}$ | $\Delta E_{exch,del}^{(2)}$/<br>kcal mol$^{-1}$ | $\Delta E^{MP2}$/<br>kcal mol$^{-1}$ |
|---|---|---|---|---|---|---|---|---|
| 2.0 | −20.241 | 90.662 | −28.594 | 41.828 | −0.753 | −11.285 | 7.900 | 37.689 |
| 2.1 | −15.234 | 68.566 | −21.133 | 32.199 | −0.633 | −9.046 | 6.251 | 28.771 |
| 2.2 | −11.443 | 51.843 | −15.682 | 24.718 | −0.527 | −7.253 | 4.926 | 21.863 |
| 2.3 | −8.585 | 39.196 | −11.684 | 18.927 | −0.436 | −5.819 | 3.874 | 16.546 |
| 2.4 | −6.438 | 29.638 | −8.739 | 14.461 | −0.358 | −4.674 | 3.043 | 12.472 |
| 2.5 | −4.829 | 22.419 | −6.564 | 11.026 | −0.292 | −3.761 | 2.390 | 9.362 |
| 2.6 | −3.626 | 16.965 | −4.950 | 8.390 | −0.237 | −3.033 | 1.877 | 6.996 |
| 2.7 | −2.725 | 12.844 | −3.748 | 6.371 | −0.192 | −2.452 | 1.474 | 5.201 |
| 2.8 | −2.052 | 9.729 | −2.850 | 4.827 | −0.155 | −1.988 | 1.157 | 3.842 |
| 2.9 | −1.547 | 7.373 | −2.177 | 3.649 | −0.124 | −1.616 | 0.909 | 2.818 |
| 3.0 | −1.168 | 5.591 | −1.670 | 2.752 | −0.100 | −1.317 | 0.713 | 2.048 |
| 3.1 | −0.884 | 4.241 | −1.287 | 2.069 | −0.080 | −1.077 | 0.560 | 1.472 |
| 3.2 | −0.669 | 3.219 | −0.998 | 1.551 | −0.064 | −0.884 | 0.439 | 1.043 |
| 3.3 | −0.507 | 2.444 | −0.778 | 1.159 | −0.051 | −0.727 | 0.344 | 0.725 |
| 3.4 | −0.385 | 1.856 | −0.609 | 0.862 | −0.040 | −0.601 | 0.270 | 0.491 |
| 3.5 | −0.292 | 1.411 | −0.480 | 0.638 | −0.032 | −0.498 | 0.211 | 0.320 |
| Fullerene-like cage | | | | | | | | |
| 2.0 | −20.300 | 89.938 | −25.300 | 44.338 | −0.397 | −11.477 | 6.781 | 39.244 |
| 2.1 | −14.287 | 63.348 | −17.372 | 31.689 | −0.314 | −8.784 | 4.998 | 27.588 |
| 2.2 | −9.975 | 44.461 | −12.011 | 22.475 | −0.247 | −6.709 | 3.657 | 19.176 |
| 2.3 | −6.918 | 31.105 | −8.356 | 15.832 | −0.193 | −5.118 | 2.661 | 13.182 |
| 2.4 | −4.769 | 21.694 | −5.845 | 11.080 | −0.149 | −3.907 | 1.926 | 8.951 |
| 2.5 | −3.453 | 15.892 | −4.321 | 8.118 | −0.118 | −3.104 | 1.455 | 6.351 |
| 2.6 | −2.358 | 11.024 | −3.054 | 5.612 | −0.089 | −2.378 | 1.045 | 4.189 |
| 2.7 | −1.604 | 7.626 | −2.173 | 3.850 | −0.067 | −1.828 | 0.748 | 2.703 |
| 2.8 | −1.086 | 5.262 | −1.557 | 2.618 | −0.050 | −1.410 | 0.534 | 1.692 |
| 2.9 | −0.734 | 3.622 | −1.126 | 1.762 | −0.037 | −1.091 | 0.379 | 1.013 |
| 3.0 | −0.494 | 2.488 | −0.823 | 1.171 | −0.027 | −0.849 | 0.269 | 0.564 |
| 3.1 | −0.333 | 1.706 | −0.608 | 0.765 | −0.020 | −0.664 | 0.190 | 0.271 |
| 3.2 | −0.224 | 1.168 | −0.455 | 0.489 | −0.015 | −0.522 | 0.134 | 0.086 |
| 3.3 | −0.150 | 0.798 | −0.346 | 0.302 | −0.011 | −0.413 | 0.094 | −0.028 |
| 3.4 | −0.107 | 0.575 | −0.276 | 0.192 | −0.008 | −0.339 | 0.069 | −0.087 |
| 3.5 | −0.072 | 0.392 | −0.215 | 0.105 | −0.006 | −0.272 | 0.048 | −0.126 |

the results presented in Table 1, the relatively low level of theory such as MP2/aug-cc-pVDZ recovers almost 85% of the total first order hyperpolarizability calculated within the CCSD(T)/aug-cc-pVQZ approach. This produces the error significantly smaller than using the large basis set within the MP2 approximation (recovers only 67% of the CCSD(T)/aug-cc-pVQZ value) or CCSD(T) approximation with the small basis set (129% of the CCSD(T)/aug-cc-pVQZ value).

## B Properties of the helium–LiH complex

The investigation of the quality of the MP2/aug-cc-pVDZ results was additionally performed for the LiH–helium complexes. Two systems were analyzed: one containing two helium atoms placed in the positions cut out from the tubular cage of the smallest radius and the other built of twenty helium atoms equivalent to the cylinder with the helium–helium distance equal to 2.5 Å. The corresponding data are collected in Tables 2 and 3. Although higher electron correlation contributions are non-negligible, the MP2/aug-cc-pVDZ approach can be applied as the tool to obtain the correct qualitative tendencies for the interaction energy and interaction-induced electric properties for the LiH–helium complexes.

**1 Interaction energy.** Fig. 2 presents the components of the interaction energy for the investigated helium systems enclosing the LiH molecule. One should notice that here is no qualitative differences between the interaction in the cylindrical and spherical system. The total interaction energy estimated both within the HF and MP2 approaches is significantly repulsive, particularly for the short intermonomer distances. The results of the interaction energy decomposition

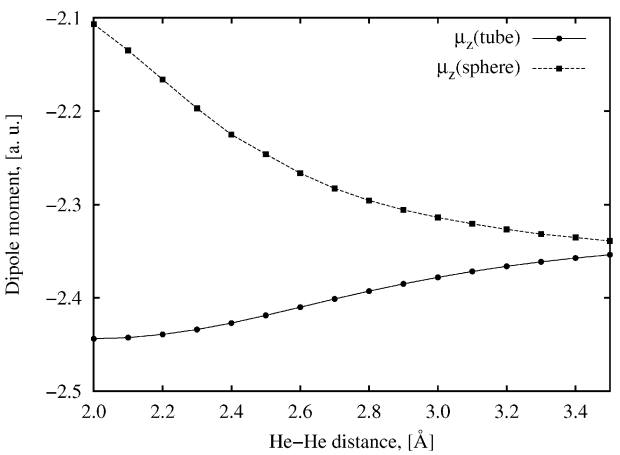


**Fig. 3** The $z$-component of the dipole moment for the tubular and fullerene-like helium–LiH complexes calculated at the MP2/aug-cc-pVDZ level of theory.

 

for both cavity shapes are summarized in Table 4. The main destabilizing contribution is the exchange energy, which is partially cancelled by the electrostatic and delocalization components in the first order. The dispersion forces of the attractive character, although not negligible, are neutralized to the height extent by the second-order exchange contribution, therefore the HF interaction energy does not differ much from the interaction energy calculated at the MP2 level of theory.

**2 Dipole moments.** The *z*-component of the dipole moment of the investigated complexes is presented in Fig. 3. Here, at first glance, one can notice the difference between the spherical and cylindrical helium cavity. The dipole moment for the centrosymmetric cavity is equal zero and for the isolated LiH molecule within the applied approach—2.349 a.u. However the enclosing of the LiH molecule in the helium cavity noticeably modifies the properties of the system causing the decrease of the absolute value of the dipole moment in the case of the spherical restriction and the increase for the tubular shape of the cage. The tendency for the cylindrical confining potential is consistent with the data obtained in the case of the 1-cyanoethyne molecule enclosed in the helium nanotube:[10] The smaller the radius of the confining cavity, the larger is the response of the complex in terms of the absolute value of the dipole moment. One should however notice that the $\pi$-electron system in the 1-cyanoethyne system is much more spatially expanded than the small LiH molecule and the confinement effects will be observed for the tubes with relatively large radius.

Fig. 4 clearly shows that the interaction-induced dipole moment for the complex with the spherical cage rises from zero for infinite radii of the confining cavities to about 0.25 a.u. for the He–He distance equal to 2.0 Å what corresponds to the radius of 2.18 Å. Simultaneously, for the potential with the axial symmetry the corresponding *z*-component of the interaction-induced dipole moment is reduced by almost 0.1 a.u. The trends obtained in the present study remain in agreement with the data presented by Klobukowski *et al.*[41] for the cylindrical potential and by Strasburger *et al.*[50] for the spherical potential enclosing the LiH molecule. The enhancement of the ionic character of the wavefunction for the axial

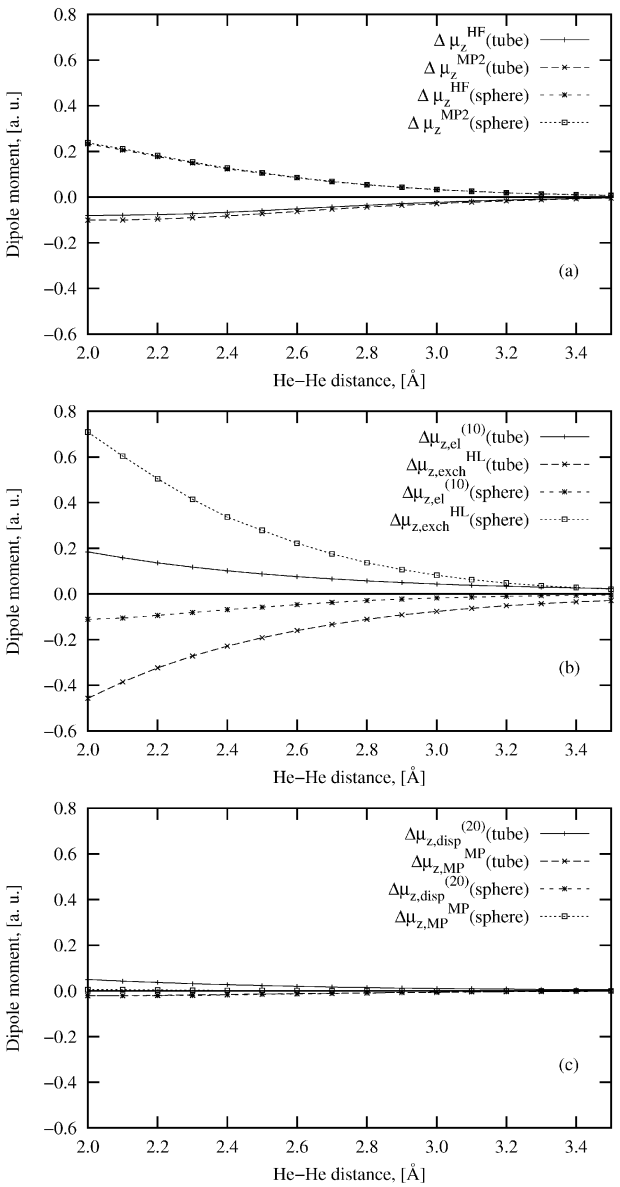


**Fig. 4** The decomposition of the *z*-component of the interaction-induced dipole moment for the tubular and fullerene-like helium–LiH complexes calculated at the MP2/aug-cc-pVDZ level of theory.

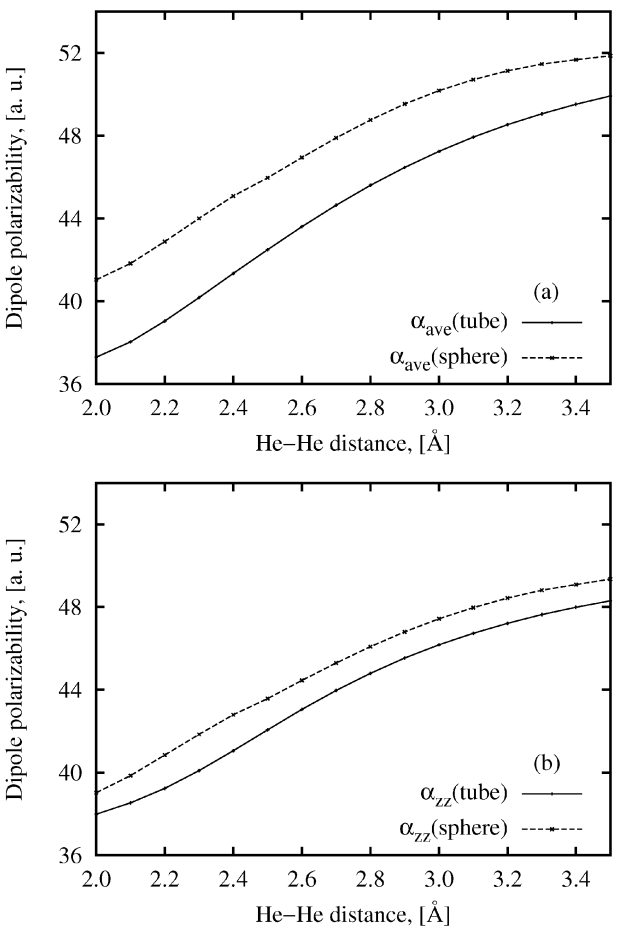


**Fig. 5** The average dipole polarizability and dipole polarizability *zz*-component for the tubular and spherical helium–LiH complex calculated within the MP2/aug-cc-pVDZ approach.

confined system generates the noticeable increase in the dipole moment of the LiH particularly for the geometries far from equilibrium.[41] The opposite tendencies—the reduction of the dipole moment together with the increasing pressure exerted by the cage is observed for the spherical model potential.[50]

The careful analysis of the components of the interaction-induced dipole moment shows that the dominant contribution in the first order is the exchange component partially cancelled by the electrostatics and delocalization increments. The second-order corrections to $\Delta\mu$ are small in the case of the tubular helium cage and negligible for the spherical enclosure. Therefore one can see that the values of the interaction-induced dipole moments calculated within the HF and MP2 approaches differ only marginally. These observations remain correct for both shapes of the helium cavities.

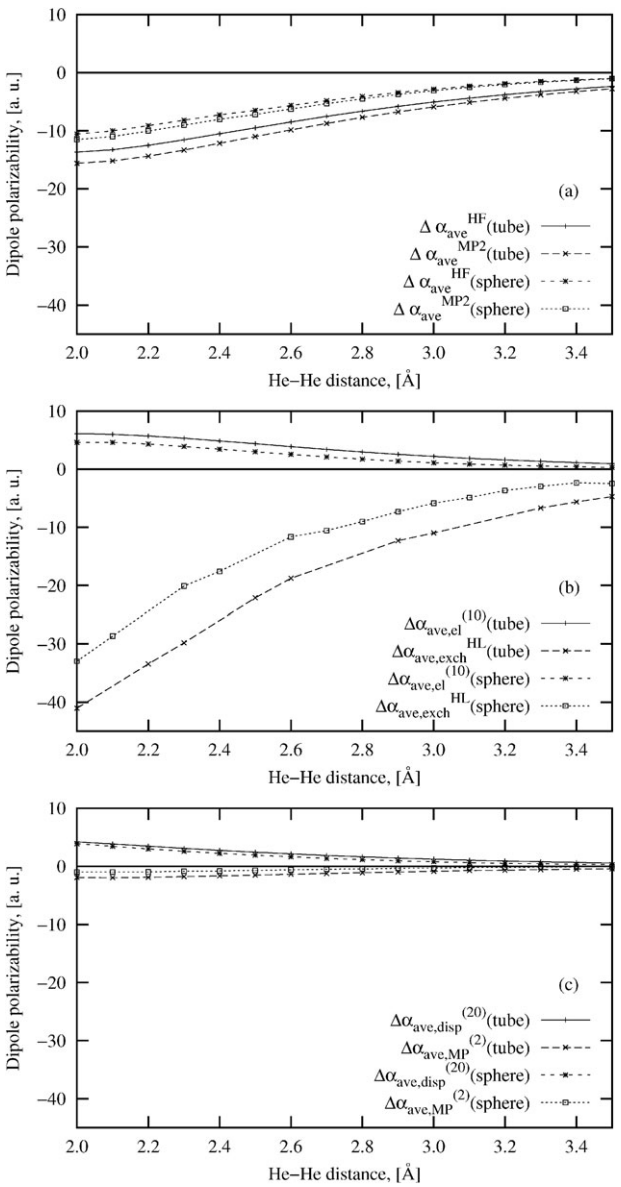


**Fig. 6** The interaction-induced average dipole polarizability components for the tubular and spherical helium–LiH complex calculated within the MP2/aug-cc-pVDZ approach.

**3 Dipole polarizabilities.** The picture of the polarizability is not as clear as for the dipole moment in the case of the LiH molecule in helium cages. This arises from the fact that the dipole polarizability of the helium cavity is non-zero. Still the comparison among the various confining helium structures is possible, since they contain the same number (twenty) of helium atoms. This was not the case in ref. 10 where the helium cavities corresponded to the tubes of various chirality: (2,2), (3,3) and (4,4), and therefore were built of 20, 30 and 40 helium atoms, respectively.

The total average polarizability of the spherical and cylindrical helium–LiH complex is plotted in Fig. 5. The monotonous functions for the average polarizability of the system and the polarizability diagonal components behave similarly for both confinement shapes. The spatial restriction brings about the decrease of the complex response understood as the absolute value of the dipole polarizability. Likewise, the parallelism of the trends for tubular and spherical cages are observed in the case of the interaction-induced components of $\alpha_{zz}$ and $\alpha_{ave}$. These findings remain correct for the total values of the polarizability at the HF or MP2 level of theory as well as for the particular components depicted in Fig. 6. Again, the main contribution is the first-order exchange term counterbalanced partially by delocalization and electrostatic

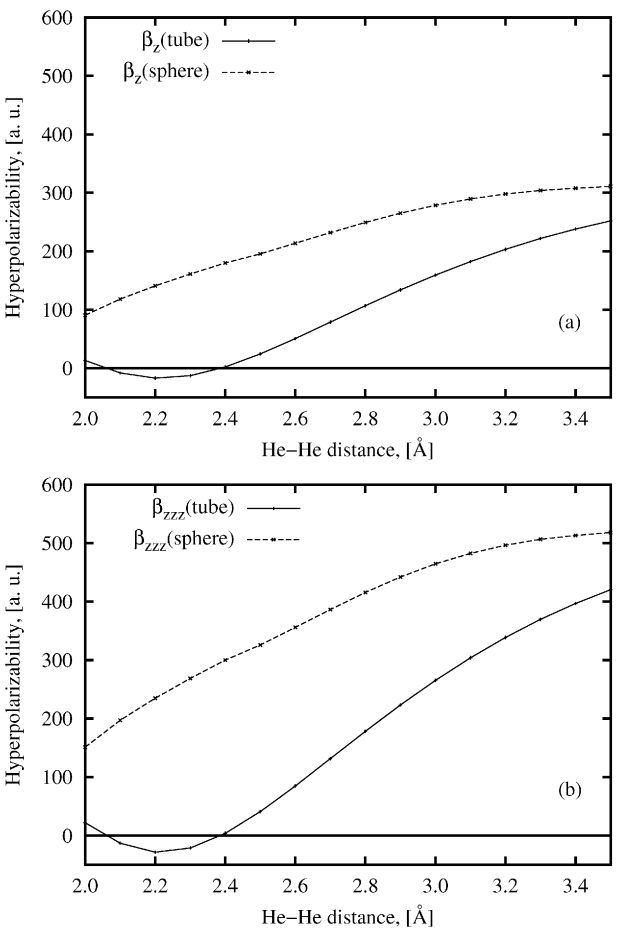


**Fig. 7** The $\beta_z$ and hyperpolarizability *zzz*-component for the tubular and spherical helium–LiH complex calculated within the MP2/aug-cc-pVDZ approach.

components. The second-order corrections amount to less than 15% of the total interaction-induced dipole polarizability for both confinement shapes at all intermolecular distances, hence even the HF values remain qualitatively correct.

**4 First-order hyperpolarizabilities.** Fig. 7 shows the general trends of the changes in the average first order hyperpolarizability $\beta_z$ and the *zzz*-hyperpolarizability component. Although for both cavity shapes the tendencies are similar in the case of the larger helium cages, for the shortest He–He distance that is equivalent to the highest pressures both spherical and cylindrical confinement effects differ. The tubular potential induces the minimum on the hyperpolarizability curve for the interhelium distances equal to 2.2 Å, that corresponds to the tube radius of 2.17 Å, while for the spherical cavities the hyperpolarizability increases monotomically for the increasing cage radius in the investigated range. The careful analysis of the interaction-induced hyperpolarizability allows to notice similar trends as for the total hyperpolarizability of the complex within the MP2 approach as well as for the HF approximation. For both methods the plots of $\beta_z$ as the function of the He–He distance are parallel. The perturbational second-order corrections stabilize the system additionally deepening the minimum for the tubular potential and enhancing the absolute value of the interaction-induced hyperpolarizability with respect to the HF data. One should also note that since the interaction-induced $\beta_z$ values are negative, (Fig. 8), the total hyperpolarizability of the complex is lowered with respect to the sum of the hyperpolarizabilities of its constituents calculated in the dimmer-centered basis set. For the centrosymmetric system such as the helium tube or sphere, the hyperpolarizability is equal to zero—only slight variation from zero is observed due to the mathematical procedure applied (DCBS). Therefore the complex hyperpolarizability arises from the guest molecule and the confining effects only. Thus it is appropriate to say that the confinement effects cause the significant decrease of the first-order hyperpolarizability of the LiH molecule.

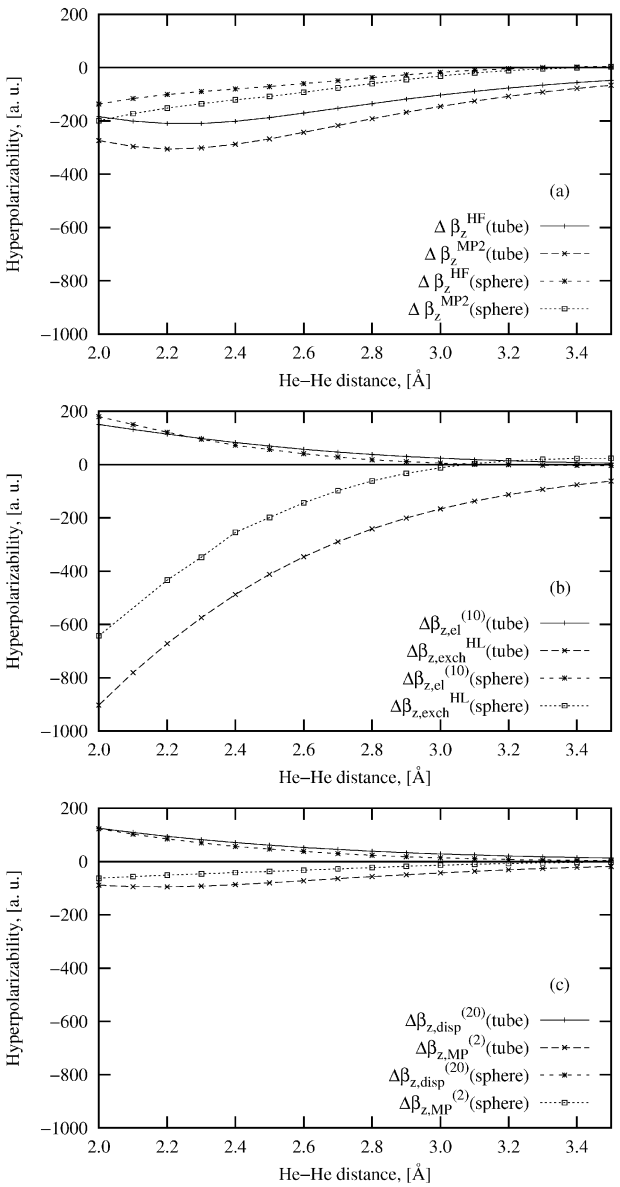


**Fig. 8** The interaction-induced $\beta_z$ hyperpolarizability component for the tubular and spherical helium–LiH complex calculated within the MP2/aug-cc-pVDZ approach.

## IV. Summary

The interaction energy of the LiH molecule with the helium cavities and the interaction-induced electric properties are discussed in the present contribution. The main force determining the properties of the helium–LiH complexes investigated here is the exchange repulsion. The dispersion contributions arising in the second order of the perturbational-variational treatment occur small, particularly in the case of the interaction-induced properties. This observation together with the earlier data allows to expect that the investigation of the similar properties for the larger systems could be reliable even at the HF level of theory. One has to remember however that the helium-embedded systems are simplified models retaining topological characteristics but neglecting the influence of the delocalized π-electron density present in the carbon nanotubes or fullerenes. Therefore they constitute the transition step from the model potentials exerting pressure on the molecular system to the real molecules enclosed in chemical (for example carbon) environments. The latter systems are much more complex and their understanding can be achieved on the basis of the informations gathered for the helium cavities. So far the data obtained for both simple models are mutually consistent, therefore now the behaviour of the model system in the carbon nanotubes and fullerenes needs to be investigated to complete the picture. All these data and the predicted tendencies are important from the point of view of the non-linear optical material design and could possibly be further utilized practically.

## Acknowledgements

The calculations have been performed in AGH Cyfronet Kraków, PCSS Poznañ and WCSS Wrocław.

## References


1 W. Jaskolski, *Phys. Rep.*, 1996, **271**, 1.
2 A. Michels, J. de and A. Bijl, *Physica A*, 1937, **4**, 981.
3 A. Sommerfeld and H. Welker, *Annu. Phys.*, 1938, **32**, 56.
4 P. V. Yurenev, A. V. Scheibinin and V. I. Pupyshev, *Int. J. Quantum Chem.*, 2008, **108**, 2666.
5 C. Díaz-García and S. A. Cruz, *Int. J. Quantum Chem.*, 2008, **108**, 1572.
6 H. E. Montgomery, *Chem. Phys. Lett.*, 2002, **352**, 529.
7 D. Bieliñska-Wąż, G. H. F. Diercksen and M. Klobukowski, *Chem. Phys. Lett.*, 2001, **349**, 215.
8 J. M. H. Lo, M. Klobukowski, D. Bieliñska-Wąż and G. H. F. Diercksen, *J. Phys. B*, 2005, **38**, 1143.
9 J. Karwowski, *J. Mol. Struct. (THEOCHEM)*, 2005, **727**, 1.
10 A. Kaczmarek, R. Zaleśny and W. Bartkowiak, *Chem. Phys. Lett.*, 2007, **449**, 314.
11 T. C. Dinadayalane, L. Gorb, T. Simeon and H. Dodziuk, *Int. J. Quantum Chem.*, 2007, **107**, 2204.
12 I. Yanov, Y. Kohlod, T. Simeon, A. Kaczmarek and J. Leszczynski, *Int. J. Quantum Chem.*, 2006, **106**, 2975.
13 J. Cioslowski, *J. Am. Chem. Soc.*, 1991, **113**, 4139.
14 R. Rungsirisakun, B. Jansang, P. Pantu and J. Limtrakul, *J. Mol. Struct. (THEOCHEM)*, 2005, **733**, 239.
15 D. A. Britz and A. N. Kholbystov, *Chem. Soc. Rev.*, 2006, **35**, 637.
16 N. A. Besley and A. Noble, *J. Chem. Phys.*, 2008, **128**, 101102.
17 M. D. Halls and K. Raghavachari, *Nano Lett.*, 2005, **5**, 1861.
18 M. D. Halls and H. B. Schlegel, *J. Phys. Chem. B*, 2002, **106**, 1921.
19 J. Cioslowski and E. D. Fleischmann, *J. Chem. Phys.*, 1991, **94**, 3730.
20 E. E. Santiso, A. M. George, K. E. Gubbins and M. B. Nardelli, *J. Chem. Phys.*, 2006, **125**, 084711.
21 P. W. Fowler and P. A. Madden, *Mol. Phys.*, 1983, **49**, 913.
22 P. B. Sorkin, P. V. Avramov, L. A. Chernozaronskii, D. G. Fedorov and S. G. Ovchinnikov, *J. Phys. Chem. A*, 2008, **112**, 9955.
23 P. W. Fowler and P. A. Madden, *Phys. Rev. B*, 1984, **29**, 1035.
24 P. W. Fowler and P. A. Madden, *Phys. Rev. B*, 1984, **30**, 6131.
25 D. Kędziera, A. Avramopoulos, M. G. Papadopoulos and A. J. Sadlej, *Phys. Chem. Chem. Phys.*, 2003, **5**, 1096.
26 S. A. Cruz and J. Soullard, *Chem. Phys. Lett.*, 2004, **391**, 138.
27 T. Sako, I. Cernusak and G. H. F. Diercksen, *J. Phys. B*, 2004, **37**, 1091.
28 A. L. Buchachenko, *J. Phys. Chem. B*, 2001, **105**, 5839.
29 O. Shameema, C. N. Ramachandran and N. Sathyamurthy, *J. Phys. Chem. A*, 2006, **110**, 2.
30 R. W. Munn, M. Malagoli and M. in het Panhuis, *Synth. Met.*, 2000, **109**, 29.
31 R. Dutt, A. Mukherjee and Y. P. Varshni, *Phys. Lett. A*, 2001, **280**, 318.
32 A. Banerjee, K. D. Sen, J. Garza and R. Vargas, *J. Chem. Phys.*, 2002, **116**, 4054.
33 P. K. Chattaraj and U. Sarkar, *J. Phys. Chem. A*, 2003, **107**, 4877.
34 R. W. Munn and P. Petelenz, *Chem. Phys. Lett.*, 2004, **392**, 7.
35 A. Borgoo, D. J. Tozer, P. Geerlings and F. D. Proft, *Phys. Chem. Chem. Phys.*, 2008, **10**, 1406.
36 M. G. Papadopoulos and A. J. Sadlej, *Chem. Phys. Lett.*, 1998, **288**, 377.
37 M. G. Papadopoulos, A. Willetts, N. C. Handy and A. E. Underhill, *Mol. Phys.*, 1996, **88**, 1063.
38 D. Tunega and J. Noga, *Theor. Chem. Acc.*, 1998, **100**, 78.
39 A. V. Shtoff, M. Rérat and S. I. Gusarov, *Eur. Phys. J. D*, 2001, **15**, 199.
40 R. Zalesny, W. Bartkowiak and B. Champaigne, *Chem. Phys. Lett.*, 2003, **380**, 549.
41 J. M. H. Lo and M. Klobukowski, *Chem. Phys.*, 2006, **328**, 132.
42 J. T. Frey and D. J. Doren, *Tubegen 3.3*, 2005, http://turin.nss.udel.edu/research/tubegenonline.html.
43 M. W. Schmidt, K. K. Baldridge, J. A. Boatz, S. T. Elbert, M. S. Gordon, J. H. Jensen, S. Koseki, N. Matsunaga, K. A. Nguyen, S. J. Su, T. L. Windus, M. Dupuis and J. A. Montgomery, *J. Comput. Chem.*, 1993, **14**, 1347.
44 H. A. Kurtz, J. J. P. Stewart and K. M. Dieter, *J. Comput. Chem.*, 1990, **11**, 82.
45 W. A. Sokalski, S. Roszak and K. Pecul, *Chem. Phys. Lett.*, 1988, **153**, 153.
46 S. M. Cybulski, G. Chalasinski and R. Moszynski, *J. Chem. Phys.*, 1990, **92**, 4357.
47 B. Skwara, A. Kaczmarek, R. W. Góra and W. Bartkowiak, *Chem. Phys. Lett.*, 2008, **461**, 203.
48 R. W. Gora, *EDS package v. 2.1.2.*, Wrocław-Jackson, 1998–2003.
49 G. Maroulis and A. Haskopoulos, *Chem. Phys. Lett.*, 2002, **358**, 64.
50 K. Strasburger and W. Bartkowiak, poster presentation on CESTC 2008, Hejnice, Czech Republic.


 